

1 Introduction

Data from the latest generation of X-ray satellites, *Chandra* and *XMM-Newton*, are forcing us to re-examine some of the basic tenets of the traditional cooling flow model. Various authors (e.g. Kaastra *et al.*, 2001; Peterson *et al.*, 2001; Tamura *et al.*, 2001) have drawn attention to the discrepancy between the predictions of the standard cooling flow model and observed spectra of cluster central regions. The expected emission lines for several important species (e.g. the Fe XVII 15 and 17 Å lines) do not seem to be present at the levels predicted by simple models. This is a trend that appears to be repeated in many clusters that have traditionally been thought to harbour cooling flows. Lines such as these are important because they are strong indicators of low-temperature ($\lesssim 1$ keV) gas. In a standard cooling flow, in which gas is cooling down to essentially zero, a significant flux is expected in such lines.

Several ideas (e.g. Fabian *et al.*, 2001; Peterson *et al.*, 2001) have been put forward to explain this discrepancy. Either something prevents the gas from cooling (despite its relatively short radiative cooling time), or the spectral signature of the cool gas must be disguised in some way. The poster discusses an idea that falls into the latter category, namely the suggestion that the intracluster medium (ICM) metals might be distributed inhomogeneously on small (unresolved) scales. This idea is no more than a minor extension of the multi-phase cooling flow model (Nulsen, 1986), which has always relied upon the coexistence of phases with different densities and temperatures at the same radius in the ICM. It merely allows the chemical composition of these phases to vary as well.

2 Equivalent Widths

As the simplest representation of an ICM in which the metals are not uniformly dispersed, consider the case of a two-component plasma consisting of metal-rich and metal-poor 'phases'. At a single, fixed temperature, such a two-component plasma is spectroscopically indistinguishable from a homogeneous plasma of some mean metallicity \bar{Z} ,

$$\bar{Z} = f_{\text{hi}} Z_{\text{hi}} + (1 - f_{\text{hi}}) Z_{\text{lo}}, \quad (1)$$

where the metal-rich phase has a metallicity Z_{hi} and accounts for a mass fraction f_{hi} , and the metal-poor phase has a metallicity Z_{lo} and a corresponding mass fraction $f_{\text{lo}} = 1 - f_{\text{hi}}$. The indistinguishability of the spectra in these two cases is a simple consequence of the fact that the strength of the continuum radiation is independent of Z , whilst that of the emission lines is directly proportional to Z (this relationship becomes more complex at ultra-high metallicities, but this is not relevant to the ICM). The reduction in the mass fraction of the enriched phase is therefore offset by the increased line strength. Alternatively, in the coronal limit, the local concentration of the heavy elements makes no difference to their radiation: a given number of heavy ions will radiate in the same way whether uniformly dispersed throughout the emitting volume or concentrated in a specific region.

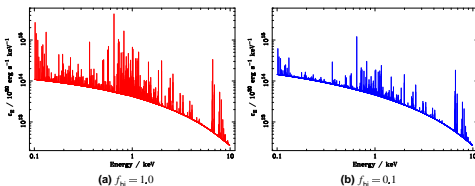


Figure 1: Spectra of isobaric cooling flows. Common parameters: $T_{\text{min}} = 10^6$ K, $T_{\text{max}} = 10^8$ K, $M = 100 M_{\odot} \text{yr}^{-1}$. (a) is for a uniform metallicity, whereas in (b) the metals are concentrated in just ten per cent of the gas.

The situation becomes more complicated (and interesting) when such a two-component metallicity plasma is allowed to cool. Shown in Figure 1 are the spectra of one- and two-metallicity plasmas. Qualitatively,

the line emission is clearly much weaker in the inhomogeneous case. Quantitatively, from the canonical expression for the spectral power of an isobaric, steady-state flow cooling from T_{max} to T_{min} at rate \dot{M} ,

$$L_{\nu} = \frac{5}{2} \frac{k_{\text{B}}}{\mu m_{\text{H}}} \dot{M} \int_{T_{\text{min}}}^{T_{\text{max}}} \frac{\Lambda_{\nu}(T)}{\Lambda(T)} dT, \quad (2)$$

it is clear that the differential emission measure at any temperature is inversely proportional to the cooling function Λ at that temperature. Making use of this formula, together with some simplifying approximations, leads to the following expression for the equivalent width ratio Δ for a narrow emission line originating from gas over a small temperature range

$$\Delta \equiv \frac{\text{EW}(2)}{\text{EW}(1)} \approx \frac{\Lambda(T, \bar{Z})}{\Lambda(T, Z_{\text{hi}})}, \quad (3)$$

with EW(2) and EW(1) the equivalent widths for two- and one-component metallicity plasmas. Two limiting cases can be considered:

- A high-temperature emission line. In this range, the cooling is approximately independent of metallicity, so that $\Lambda(T, Z_{\text{hi}}) \sim \Lambda(T, \bar{Z}) \sim \Lambda(T, 0)$. Therefore $\Delta \rightarrow 1$, i.e. there is no change in the equivalent width of a high-temperature line.
- A low-temperature emission line. In the regime where the cooling is dominated by metals, we can show that $\Delta \rightarrow f_{\text{hi}}$.

In practice, for lines existing at intermediate temperatures, or over a non-negligible range of temperatures, behaviour intermediate between these limits is expected, as shown in the following figure. This quantifies the degree of suppression of the equivalent width that can be obtained for various spectral lines from a two-metallicity ICM, as the degree of enrichment is varied. $f_{\text{hi}} = 1.0$ corresponds to a uniform plasma, and lower values to an increasingly segregated ICM.

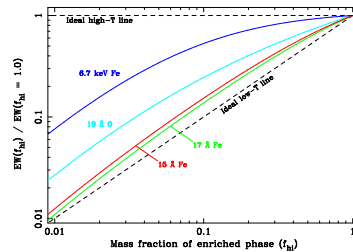


Figure 2: Effect of changing enrichment fraction on the equivalent width of some important ICM spectral lines, for a two-component metallicity ICM.

3 Time Evolution of the ICM — Abundance Profiles

We have used a simple one-dimensional numerical model of the ICM to investigate the effects that small-scale metallicity variations can have on the evolution of the intracluster gas. The code is a Lagrangian, grid-based one, in which each radial zone can have a different set of abundances. The system is allowed to evolve under the influence of gravity (in an NFW potential well) and radiative energy-loss, with the MEKAL plasma code being used to model the gas radiation. Zones that cool out of the X-ray waveband are removed from the simulation.

Cylindrical lines-of-sight are projected through the cluster at various stages in the evolution, and integrated along in order to find the spectral surface brightness of the gas at each projected radius. Integrating over a range of projected radii returns the emission spectrum of an annulus co-centric with the cluster. The radiation from each annulus is then redshifted and convolved with the appropriate instrument response function (using XSPEC), producing simulated observations incorporating Poisson noise. These are then analysed using standard observational methods. The following figure shows the results of one

particular simulation for an (initially isothermal) 10^8 K cluster in which the metals are concentrated in 10 per cent of the gas and the average metallicity is $0.3 Z_{\odot}$.

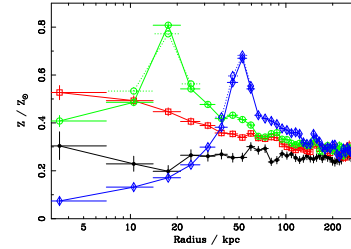


Figure 3: Time evolution of the observed abundance profile for a two-metallicity ICM. 90 per cent of the gas is metal-free, the other ten per cent is enriched to $3 Z_{\odot}$. Vertical error bars are 1σ , horizontal bars show the extent of the spectral annuli. The different curves represent different times: black filled circles 0.0 Gyr; red open squares 1.0 Gyr; green open circles 1.2 Gyr; blue open diamonds 1.6 Gyr. Results are for single temperature mekal models fitted to the 0.3–7.0 keV *Chandra* ACIS-S spectral range. Dotted lines are the results of two temperature fits, shown where the reduced χ^2 for the single temperature fits exceeded 2.0. The simulated observation time was 25 ks.

As the system evolves, the metal-rich gas cools much more swiftly than the metal-poor gas, due to its enhanced cooling function. The effect is naturally strongest in the central regions where the density is highest and the two-body bremsstrahlung radiation is most intense. This differential cooling has marked effects upon the measured abundance profile, as is clear from Figure 3. As time passes, there is a gradual increase in the derived abundances, particularly in the central regions (for example, after 1.0 Gyr the measured value for the central abundance begins to decrease again, leading to the situation where there is a peak in the abundance profile at an off-centre position. This peak declines in magnitude and moves outward with subsequent evolution. Such an abundance profile is very similar to those seen recently in *Chandra* observations of some clusters, as shown in Figure 4, which compares the observed abundance profile of Abell 2199 (Johnstone *et al.*, 2002) with one particular simulation output.

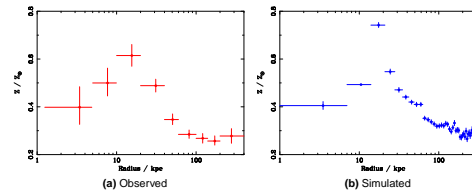


Figure 4: Comparison of observed and simulated abundance gradients. (a) *Chandra* abundance profile of A2199 — corresponds to figure 5 of Johnstone *et al.* (2002). (b) abundance profile obtained from simulated observations.

This behaviour may be explained as follows. In the simulations, the metal-rich gas (contributing the emission lines) cools relatively quickly and enters the regime where line emission is more important, whereas the metal-poor gas (contributing the bulk of the continuum) cools much more slowly. The combined consequence of these two processes is an increase in the strength of the lines relative to the continuum, that is, an increase in the equivalent width of the lines. It is essentially from the equivalent width that the fitting procedure obtains the plasma abundance. One could view this as a form of emission-weighting — as the metal-rich regions cool, the intensity of their emission increases, so

they increasingly dominate the spectral fits. The decrease in the central abundance at late times occurs as metal-rich gas there cools out of the X-ray regime and is lost from sight.

3.1 Behaviour of Individual Elements

We have also investigated the behaviour of individual elements using mekal fits to the data. The degree to which an abundance peak develops depends on how the emission lines dominating the fit for that element evolve with temperature. A strong peak is produced if the equivalent width of the emission line is a strong function of temperature (e.g. Fe L). If the change in equivalent width with temperature is weaker (e.g. Fe K), then the resulting abundance peak is less pronounced. This has consequences for the observed element ratios, as illustrated in Figure 5(b).

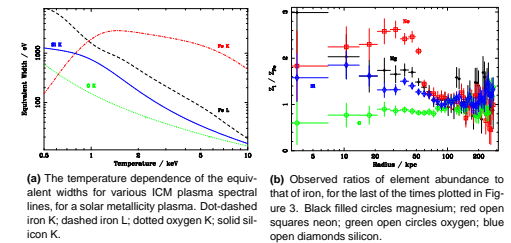


Figure 5: Behaviour of individual elements.

4 RGS Spectra

Finally, the following figure shows the effect on the *XMM-Newton* RGS spectrum of the cluster central regions in one particular simulation.

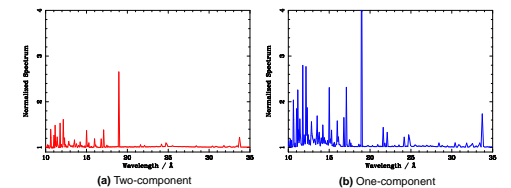


Figure 6: Spectra observed from the central Mpc of the two-metallicity cluster of Figure 3 at late times, compared with that of a one-metallicity ICM. The wavelength range is that of the *XMM-Newton* RGS instrument, and has been deredshifted. The spectra have been normalized by dividing by a fitted continuum, so that the changes in line strength are more readily apparent.

References

- Fabian A. C., Mushotzky R. F., Nulsen P. E. J., Peterson J. R., 2001, MNRAS, 321, L20
Johnstone R. M., Allen S. W., Fabian A. C., Sanders J. S., 2002, MNRAS, 336, 299
Kaastra J. S., Ferrigno C., Tamura T., Paerels F. B. S., Peterson J. R., Mitzak J. P. D., 2001, A&A, 365, L99
Nulsen P. E. J., 1986, MNRAS, 221, 377
Peterson J. R., *et al.*, 2001, A&A, 365, L104
Tamura T., *et al.*, 2001, A&A, 365, L87

For more details of the work discussed in this poster, see:

- Morris R. G., Fabian A. C., 2003, MNRAS, 338, 824.

Glenn Morris, gmorris@ast.cam.ac.uk, June 2003.